Original Research Article

Synthesis, characterization and cytotoxic activity of N-(5-indanyl(methylene)anthranilic acid(5-indanyl methylene)-hydrazide and its Pt(II) complex

Abstract A new platinum complex of N-(5-indanyl(methylene)anthranilic acid(5-indanyl methylene)-hydrazide (HL) has been synthesized and characterized by physical and spectral techniques, as elemental analysis, IR, EI-MS, ^{1}H-NMR, thermal analysis, transmittance electron microscope (TEM) and magnetic moment. The results indicated that the ligand binds to Pt(II) in the enol form. Square-planar stereochemistry was suggested for the Pt(II) complex. The morphological characterization showed nano-sized spherical particles with average size 92 nm of the isolated complex. The synthesized Pt(II) complex exhibited a significant cytotoxic activity against HCT116 and HEPG2. Also *in vivo* study of the Pt(II) complex showed cytotoxic activity towards Ehrlich ascites carcinoma (EAC).

Keywords Synthesis. Pt(II) complex. Cytotoxic activity

Introduction

Cancer is the major serious problem which causes death all over the world. The cause of cancer is attributed to genetic damage to the cells. The damaged cells do not respond to normal tissue controls. The affected cells multiply rapidly to cause spread of cancer and formation of varying degrees of tumors (Zhukova and Dobrynin, 2001).

The discovery of effective new cancer therapies is a strong demand. Since the discovery of the platinum based complex, cisplatin, in 1965 (Divsalar et al., 2013), medicinal inorganic chemistry has attracted much more attention and a large number of platinum complexes with promising pharmacological properties have been synthesized (Kostova, 2006). The cytotoxic action mechanism of many metal complexes has been discussed aiming to develop new anti-tumor agents (Grunicke et al., 2006; Noordhui et al., 2008; Chang et al., 2015; Wei et al., 2014, Sönmez M. et al., 2010). The presence of metal centers capable of binding to negatively charged bio-ligands, as proteins and nucleic acids offers the metal complexes excellent potential pharmaceutical properties (Sakurai et al., 2002; Jian et al., 2010). The metal complex is considered a chemotherapeutic agent in cancer treatment, when it slows and stops the cancer from spreading by killing the rapidly

dividing cells. In chemotherapy, the target is to kill the tumor cells, without causing damage to the healthy cells. Cisplatin and carboplatin have been used in the treatment of various cancers as chemotherapeutic agents (Kostova, 2006). Serious side effects accompany the use of these drugs, so, trials are done to find new platinum complexes with less toxicity, to be used as potential anti-cancer agents (Ehrsson et al., 2002). As a result, new platinum complexes with different organic ligands have been designed (Al Jibori et al., 2014; Tabrizi and Chiniforoshan, 2017., Wang et al., 2015; Wang et al., 2017).

In this paper a new Pt(II) complex of a hydrazide derivative N-(5-indanyl(methylene)anthranilic acid (5-indanyl methylene)-hydrazide has been synthesized and characterized by various techniques. The cytotoxic effect of the synthesized Pt(II) complex was studied.

To the best of our knowledge no work has been carried out on the present ligand, only a patent described the synthesis, the anti-inflammatory and analgesic activity of similar derivatives N-(substituted-naphthyl-1) anthranilic acid, was presented (Fujio and Tomoaki 1976).

Materials and methods

N-(5-indanyl(methylene)anthranilic acid(5-indanyl methylene)-hydrazide and $PtCl_2$ were purchased from Sigma-Aldrich (S512095). ^{1}H-NMR of the ligand in DMSO-d_6 δ (ppm): 2.0 (m, 2H, CH_3), 2.49 (t, 4H, C_5-2H), 2.8 (t, 2H, 2H). CH=N appears at 6.8 (s, 1H), 7.43-7.8 (m, 10H).

Instruments

The elemental analysis, C, H and N were carried in the instrumentation center, Granada University, Spain, on Thermo Scientific Flash 2000 Analyzer. TGA (thermo-gravimetrical analysis measurements) were carried out on a Shimadzu model 50 H instrument with nitrogen flow rate 20 cm^3/min., and heating rate 10 ^oC/min. Magnetic measurements were carried out on a Sherwood Scientific Magnetic Balance. The ^{1}H-NMR spectra in DMSO-d_6 were carried out on a 500 MHz JEOL spectrophotometer. Fourier-transformer infrared spectra (FT-IR) were carried out as KBr discs on a Mattson 5000 FTIR spectrometer. EI-MS was recorded on spectrometer WATERS modelo SYNAP G2 in instrumentation center, Granada University, Spain. CM 20 PHILIPS electron microscope was used to take the transmittance electron microscope (TEM) images.

Synthesis of Pt(II) complex

0.001 M (0.265 gm) of $PtCl_2$ in 10 ml ethanol was injected to 0.001 M (0.40 gm) of (N-(5-indanyl(methylene)anthranilic acid (5-indanyl methylene)-hydrazide in 25 ml hot ethanolic solution under nitrogen. A yellow precipitate was formed on reflux. The reaction mixture was refluxed for 3 hrs and the precipitate was filtered off under vacuum.

The trials to obtain a single crystal from the platinum complex was failed, unfortunately, the diffraction pattern indicated that the isolated complex is amorphous.

Yellow powder (yield 55%); m.p. >300 °C. Anal. Calc. for $PtC_{54}H_{57}N_6O_{6.5}$: C, 59.6; H, 5.3; N, 7.7; Pt, 17.9% Found: C, 60.0; H, 5.4; N, 7.3; Pt, 18.1 %.

Pharmacological testing

In vitro study (Cytotoxicity)

Cytotoxic activity of Pt(II) was performed on a panel of human tumor cell line HEPG2 (hepatocellular carcinoma), HCT 116 (human colon cancer) at different concentrations. The method of Philp et al was used to carry out the cytotoxicity as sulphorhodamine-B(SRB) assay (Philips *et al.*, 1990). SRB is a protein stain in mild acidic conditions. This stain is used to provide a sensitive index of cellular protein content. It is a bright pink ammoxanthrene dye with two sulphonic groups.

In vivo study (Toxicity studies)

LD50 of Pt(II) complex in mice was determined according to the method of Meier and Theakston (Meier and Theakston 1986).

Dose response

Dose response of Pt(II) complex was determined in mice according to the method described by Crump et al (Crump et al., 1976). Animal care and experiments were performed in accordance with NIH guide to the care and use of laboratory animals.

Experimental design: 20 female Swiss albino mice were divided into two groups (10 mice per each group): Group I is the positive control and injected intraperitonealy with $2.5x10^6$ of Elhrlich ascites carcinoma "EAC" cells. Group II is the Pt(II) complex therapeutic group, injected intraperitonealy with $2.5x10^6$ of Elhrlich ascites carcinoma "EAC" cells, and after one day of EAC injection, therapeutic group injected intaperitonealy with 5 mg/kg of Pt(II) complex day after day. At the end of the experiment, EAC cells were collected from mice and viability study was assayed.

Cell viability and counting of EAC cells

Trypan blue exclusion method (McLiman et al., 1957) was used to determine the counting and viability of EAC cells. The total and viable cells (nonstained) were determined in the two groups as the number of cells /ml at magnification power X40.

Statistical analysis

SPSS software version 14 (Levesqiue 2007) was used to perform statistical analysis. One way analysis of variance was used to assess using the effect of each parameter. The results were presented as mean ± SD. Analysis of variance (ANOVA test), was used to determine the differences between mean values followed by Duncan's multiple rank test using MSTAT-C computer program.

From linear regression analysis the statistical significance (where P≤ 0.05 was considered significant) of the relationships between variables was calculated.

Results and discussion

IR spectra of the ligand and its Pt(II) complex

Two tautomeric forms are suggested for the ligand, the Keto (Fig.1 A) and the enol (Fig.1B). The keto form (1A) is the major tautomer in the solid state. The formula $[Pt(L)_2]4.5H_2O$ represents the complex formed from the reaction of (N-(5-indanyl(methylene)anthranilic acid (5-indanyl methylene)-hydrazide and $PtCl_2$. The ligand chelates the Pt(II) ion in the enol form after displacement of hydrogen ion from the enolic carbonyl (Fig. 2).

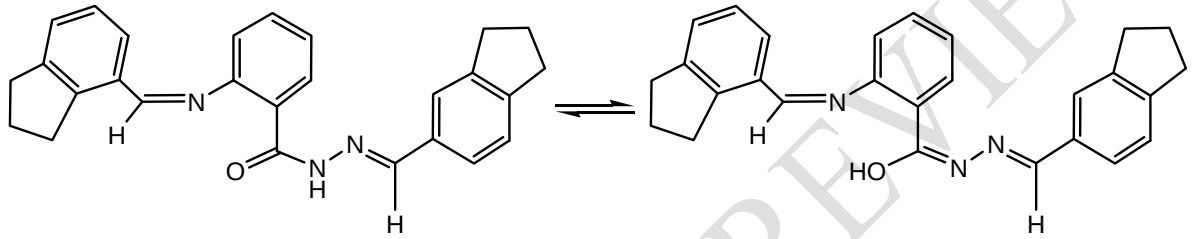

(A) keto form (B) enol form

Fig.1. The two possible tautomeric forms of the ligand.

The isolated Pt(II) complex is stable in air, soluble in coordinating solvents as DMF and DMSO, but insoluble in water. The elemental analysis indicated that the isolated Pt(II) complex is pure compound.

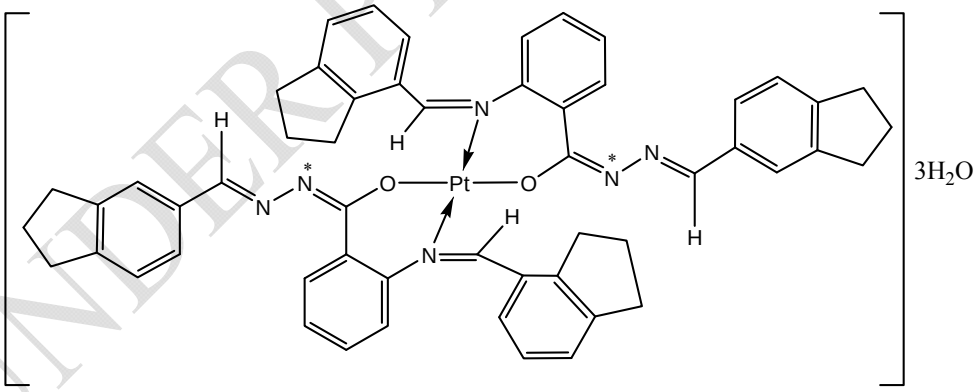

Fig. 2. Suggested structure of Pt(II) complex

Some important IR bands of the ligand and its Pt(II) complex with their probable assignments are indicated in Table 1. The ligand exhibits strong band at 3286 cm^{-1} due to ν (NH). The strong bands at 1662 and 1621 cm^{-1} are attributed to ν (C=O) and ν (CONH), respectively (Nakamoto, 1970; Hosny and Sherif 2015; Hosny (2009); Hosny and Shallaby (2007). These bands confirm the presence of the free ligand in the keto form. The ligand shows also, bands at 1605,

1306, 1199 and 971 cm^{-1} attributed to ν (HC=N), ν (C-O), ν (C-N) and ν (N-N), respectively (Nakamoto, 1970; Hosny, 2010). Comparison of the IR spectrum of the ligand with that of Pt(II) complex reveals that the ligand chelates Pt(II) ion in a mono-negative bidentate mode *via* azomethine nitrogen (C=N) and the enolized carbonyl oxygen after displacement of hydrogen (Fig. 2). The disappearance of the strong bands assigned to ν(NH), ν(CO) and ν(CONH) in the free ligand and the appearance of a new medium band at 1650 cm^{-1} assigned to ν (C=N*) in the spectrum of Pt(II) complex support the suggested chelation mode. There is other possible coordination mode which may exist for the ligand, including formation of 5-membered chelate ring through N-N=CH group. This latter mode was discarded on the basis of the remaining of the bands at 969 and 1605 cm^{-1} due to ν (N-N) and ν (HC=N) unaltered in comparison with its position in the spectrum of the organic ligand. The remaining of these bands unaltered, confirms the inertness of N-*N active sites towards coordination (Nakamoto, 1970). The presence of hydrated water in the Pt(II) complex is confirmed by the presence of bands at 3431, 746 and 690 cm^{-1} due to ν (OH), δ (OH) and ρ_w (OH), respectively (Misbahur Rehman, 2017; Hussien et al.,2015; Hosny et al., 2014). New weak bands are observed at 557 and 449 cm^{-1} due to ν (M-O), ν (M-N) respectively (Hosny 2007; Sherif and Hosny, 2014).

Table1. IR spectral data in (cm^{-1}) for the ligand (HL) and its Pt(II) complex.

Compound	ν(NH)	ν(C=O)	ν(C=N*)	ν(C=N)	ν(C-O)	ν(C-N)	ν(M-O)	ν(M-N)
The ligand (HL)*	3286	1662	-	1605	1306	1199	-	-
$[Pt(L)_2]3H_2O$	-	-	1650	1603	1292	1144	557	445

* HL = (N-(5-indanyl(methylene)anthranilic acid (5-indanyl methylene)-hydrazide

Pt(II) complex may exist either in N-N *(cis),* O-O*(cis)* or N-N*(trans),*O-O *(trans)*. Molecular mechanics method was used to predict rapidly the geometries of the two suggested conformers by using hyperchem series of programs (Hyperchem 7, 2002). The total energy calculations of the two structures indicated that the *trans* form is only 2 KJ mol^{-1} more stable than the *cis* form.

^{1}H-NMR

^{1}H-NMR spectrum of the ligand (N-(5-indanyl(methylene)anthranilic acid (5-indanyl methylene)-hydrazide in DMSO-d_6 shows signals attributed to cyclopentane ring at *δ* 1.92-1.99 (m, 4H, $2CH_2$) and 2.75-2.86 (m, 16H, $6CH_2$, 4CH). Three singlet signals appear at *δ* 6.42, 7.55, 8.73 ppm due to the protons of secondary amine NH, two azomethine protons (C**H**=N) and C**H**=N-NH, respectively. The multiplet signals integrated for 6 protons resonate around 675 and 7.29-7.54 ppm characteristic

for cyclohexadiene olefinic protons. The four aromatic protons of the benzene ring are observed in the region 7.13-7.27(m, 2H, Ar-H) and (m, 2H, Ar-H).

^{1}H-NMR spectrum of Pt(II) complex taken in DMSO-d_6 reveals beside the expected signals of cyclopentane ring, cyclohexadiene olefinic protons in the range 1.99-3.80 ppm and the aromatic protons in 6.70-7.50 ppm. The absence of the NH signal which appears at δ 6.42 ppm in the spectrum of the free ligand was attributed to the enolization of the carbonyl with subsequent liberation of this proton on coordination to the Pt(II) ion. The singlet signal of the azomethine (C**H**=N) resonates downfield at δ 8.00 ppm. This shift in the signal position supports the participation of the azomethine group in complex formation.

Mass spectra

The EI-MS of Pt(II) complex (Fig. 3) exhibits the molecular ion peak at *m/z* = 1087, in agreement with the formula $[Pt(C_{27}H_{23}N_3O)_2]4.5H_2O$ after removal of H_2. Two possible pathways have been suggested for the fragmentation of Pt(II) complex (Scheme 1). The molecular ion peak may lose four and half water molecules and the fragment [PtL] to give a peak at *m/z* = 406, assigned to the free ligand. The free ligand is fragmented by loss of propene and methane molecule by special rearrangement to give the peak at *m/z* = 346. The last peak is further fragmented by loss of carbon monoxide and nitrogen giving the base peak at *m/z* =304. The base peak loses hydrocyanic acid and nitrogen forming the peak at *m/z* = 263. In the second pathway, it was suggested that the molecular ion peak loses three and half molecules of water forming the peak at *m/z* = 1027. The latter peak is fragmented by lose of water molecule and the fragment C_6H_3 giving the peak at *m/z* = 935. The latter peak loses tropyllium and furayl groups to give the peak at *m/z* = 778. The peak at *m/z* = 778 is further fragmented by loss of benzene and butadiene to give the peaks at *m/z* = 701 and 648, respectively. The last fragment loses butane to produce the fragment at *m/z* = 594, which loses hydrocyanic acid, carbon monoxide and nitrogen producing the fragment *m/z* = 525. The last fragment at *m/z* = 525 loses methane, ethylene and benzene leading to the peak corresponds to the free ligand at *m/z* = 407.

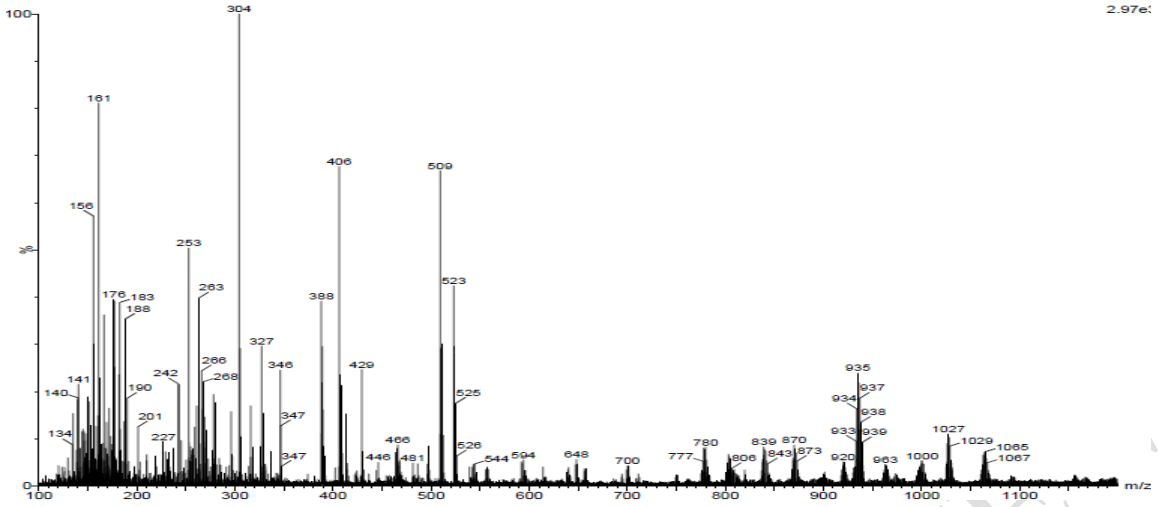

Fig. 3 . MS of Pt(II) complex

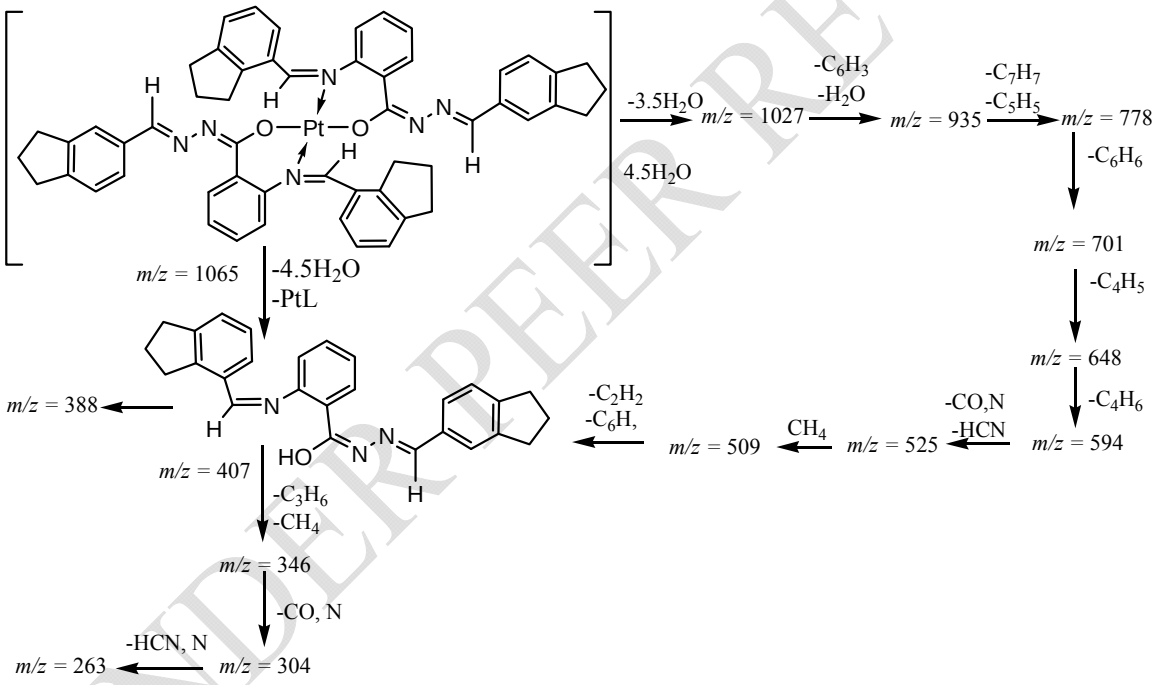

Scheme1. Fragmentation pattern of Pt(II) complex

Magnetic measurements

The Pt(II) complex is diamagnetic which confirms the formation of a square–planar stereochemistry around the Pt(II) ion (Lever, 2002).

Thermal analysis

TGA measurements of Pt(II) complex were carried out from 25 ^{o}C up to 1000 ^{o}C. The thermogram exhibits three events. The first resulted from the removal of water of hydration. This step starts from 25 ^{o}C to 140 ^{o}C. The next step was attributed to the loss of two phenyl and

four benzocyclopentane rings. This step takes place from 141 ^{o}C to 480 ^{o}C. (Found mass loss of this step is 55.5%, while the calculated mass loss is 57.0%). The last step starts from 461 ^{o}C to 880 ^{o}C, corresponding to the loss four hydrocyanic acid molecules (Found mass loss of this step is 8.7%; Calcd 9.0%).

The thermodynamic parameters of decomposition were calculated by applying Coats-Redfern (Coats-Redfern, 1964) equations. The energy of activation (E^*) and the order of the reaction (n) were determined graphically. The thermodynamic parameters E^*, ΔH^*, $\Delta G^*$and ΔS^* were calculated from equations (1-3) and found to be 10.5, 4.7, 217 KJ and -301.7 S^{-1}, respectively:

$$\Delta S^* = 2.303\ [\log (Zh/KT)]R \quad (1)$$

$$\Delta H^* = E - RT \quad (2)$$

$$\Delta G^* = \Delta H^* - Ts\ \Delta S^* \quad (3)$$

(Where, Z, h and K are the pre-exponential factor, Plank and Boltzmann constants, respectively (Sherif and Hosny, 2014). The thermodynamic parameters were calculated for the second step, which is suitable for kinetic analysis, where there is no overlapping with other steps. The positive enthalpy and free energy values reveal the endothermic and non-spontaneous decomposition of this step, respectively. The negative entropy value indicates that the structure of the activated complex is more ordered than the reactants (Sherif and Hosny, 2014).

Morphological characterization

The chemical and biological activities of metal complexes were related to their particles size and shape (Hussain and Chakravrty,2012; Hosny et al., 2015). Transmittance electron microscope (TEM) was used to determine the particles shape and size of Pt(II) complex. From the TEM images (Fig.4), it is clear that the particles of Pt(II) complex are spherical in shape.

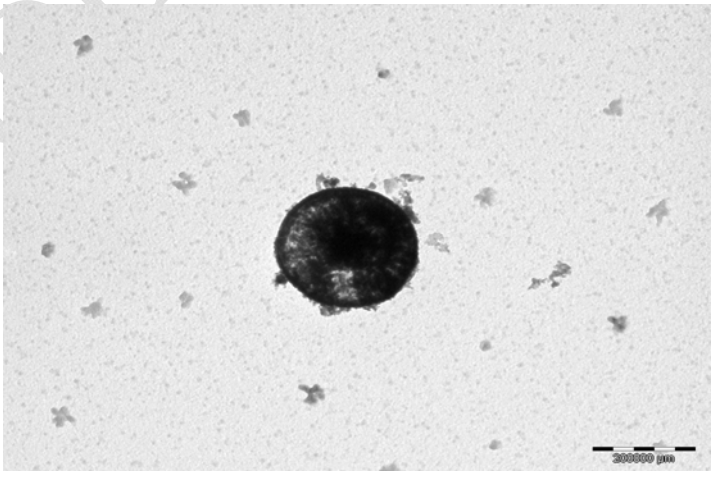

Fig. 4. TEM images of Pt(II) complex

The possible formation mechanism of the spherical particles of Pt(Indanyl) complex has been proposed as indicated in Scheme 1. Under reflux conditions, the soluble Pt^{2+} cation reacts with the indanyl ligand to form insoluble Pt(Indanyl) nucleus. In the first stage, Pt(Indanyl) complex follows a heterogeneous nucleation, where the energy barrier is lower than nucleation in solution (Luo et al., 2011; Mohammadikish 2014). Initially, large numbers of small primary nanoparticles are formed. These primary particles have high surface energy, which makes them unstable. They aggregate rapidly and grow forming spherical nanoparticles. The nanospheres are assembled to each other via random attachment to reduce the surface energy forming thermodynamically stable structure. Finally, spontaneous aggregation takes place in spherical form to minimize the surface area.

Biological Study

Cytotoxicity

The in vitro cytotoxic activities of Pt(II) and the standard doxorubcin were shown in Table 2 and Figs 5, 6. The minimum inhibitory concentration of the synthesized compound was found to be 5.3 µg/ml and 9.68 µg/ml against HCT116 and HEPG2 cell lines, respectively. The colorimetric cytotoxicity tests showed that the Pt(II) complex has in vitro cytotoxic activity against the examined cancerous cell lines with IC_{50} values of 9.08 µM and 5.43 µM against HCT116 and HEPG2 cell lines, respectively. The current results revealed that the present Pt complex inhibits cell proliferation in the same range as cisplatin and oxaliplatin.

Table 2. Minimum inhibitory concentration of doxorubicin and synthesized Pt(II) complex against HCT116 and HEPG2 cell lines

	HCT116	HEPG2
Doxorubicin	5.3 µg/ml	5.18 µg/ml
Pt (II) complex	9.68 µg/ml	5.78 µg/ml

Determination of median lethal dose (LD50) of Pt(II) complex

The results revealed that, dose up to 100 mg/kg body weight was considered safe, where no mortality was observed. Table 3 summarizes the effect of Pt(II) complex on EAC cells volume and count.

Table 3. Effect of Pt (II) complex on the volume and count of EAC in the studied groups:

Parameter	Positive control	Pt(II) complex
Volume of Ascites fluid(ml)	3.9 ± 0.11	2.24±0.18
% change	-	42.56%
Count of EAC cells ($x10^6$)	55.4 ± 0.32	26.3 ± 0.64
% change	-	52.53%

The results indicate mean volume of EAC of the positive control group is 3.9 ml. This value was significantly decreased by 42.5% in Pt(II) complex treated group ($P< 0.05$). Also, it was found that the mean count of EAC cells in the positive control group is $55.4x10^6$ which was significantly decreased in Pt(II) complex treated group, compared to the positive control group.

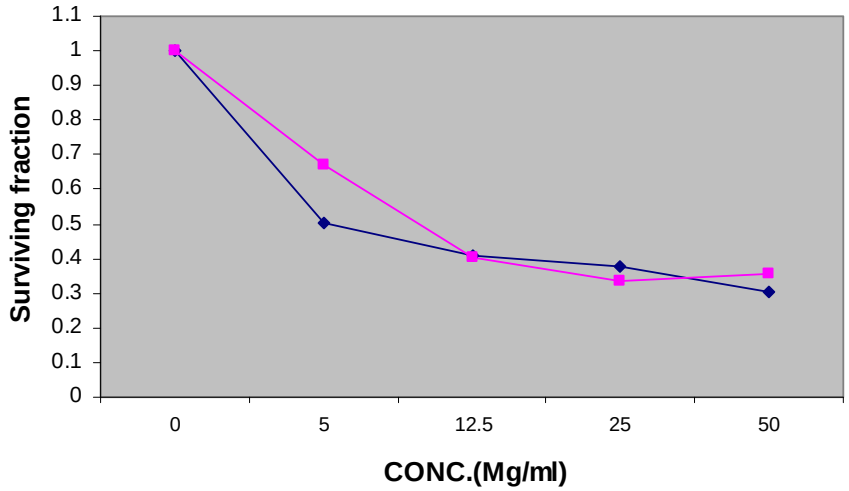

Fig. 5. Minimum inhibitory concentration of Pt(II) complex (pink) and doxorubicin (blue) against HCT cell line

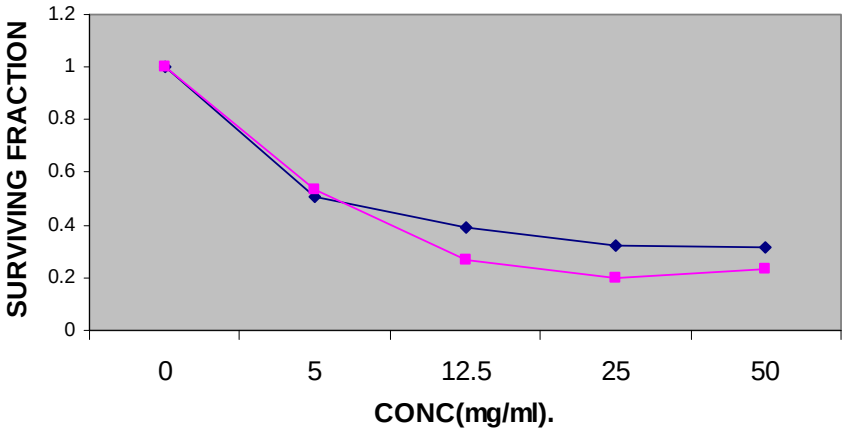

Fig. 6. Minimum inhibitory concentration of Pt(II) complex (pink) and doxorubicin (blue)against HEPG2T cell line

Conclusion

To the best of our knowledge no work has been carried out on the ligand N-(5-indanyl(methylene)anthranilic acid(5-indanyl methylene)-hydrazide and its metal complexes. The Pt(II) complex of this ligand has been synthesized and characterized by different techniques. The ligand coordinates to the Pt(II) ion in the enol form as mono-negative bidentate forming square-planar complex. TEM images indicated that the particles of Pt(II) complex exist as spherical nanoparticles. The Pt(II) complex exhibits activities on four human cancer cell lines HEPG2 and HCT 116 with IC_{50} = 1.4–9.6 μM. The activity of the Pt(II) complex was compared with some standard platinum complexes as cisplatin and carboplatin complexes.

References

Al-Jibori S. A., Al-Jibori G. H., Al-Hayaly L. J., Wagner C., Schmidt H., Timur S., Barlas F. B., Subasi E., Ghosh S., Hogarth G. 2014. Combining anti-cancer drugs with artificial sweeteners: Synthesis and anti-cancer activity of saccharinate (sac) and thiosaccharinate (tsac) complexes *cis*-[Pt(sac)$_2$(NH$_3$)$_2$] and *cis*-[Pt(tsac)$_2$(NH$_3$)$_2$], Journal of Inorganic Biochemistry, 141: 55. doi:10.1016/j.jinorgbio.2014.07.017

Coats A. W., Redfern J. P. (1964) Kinetic parameters from thermogravimetric. Nature, 201:68. doi:10.1038/201068a0

Crump K. S., Hoel D. G., Langley C. H., Peto R. 1976. Fundamental carcinogenic processes and their implications for low dose risk assessment. *Cancer Research,* 36:2973. **doi:** Published September 1976

Divsalar A., Zhila I., Saboury A. A., Nabiuni M., Razmi M., Mansuri-Torshizi H. 2013. Cytotoxic and spectroscopic studies on binding of a new synthesized bipyridine ethyl dithiocarbamate Pt(II) nitrate complex to the milk carrier protein of BLG. *Journal of Iranian Chemical Society*, 10: 951. DOI 10.1007/s13738-013-0232-6

Ehrsson H., Wallin I., Yachnin J. 2002. Pharmacokinetics of oxaliplatin in humans. *Medical Oncology*, 16: 261. doi:10.1385/MO:19:4:261

Foltinova V., Svihalkova L. S., Horvath V., Sova P., Hofmanova J., Janisch R., Kozubík A. 2008. Mechanism of effects of Pt(II) and (IV) complexes. Comparison of cis platin and oxaliplatin with satraplatin and LA-12, new platinum (IV) based drugs. A mini review. *Scripta Medica (BRNO),* 81:105.

Fujio N., Tomoaki F. 1976. Substituted naphthyl anthranilic acids. *United States Patents,* 3989746A.

Grunicke H., Doppler W., Helliger W. 1986. Tumor biochemistry as basis for advances in tumor chemotherapy. *Archive Geschwulst forsch*, 156:193. PMID:3488047

Hosny N. M. 2007. Synthesis, characterization, theoretical calculations and catalase-like activity of mixed ligand complexes derived from alanine and 2-acetylpyridine. *Transition Metal Chemistry*, 32: 117. doi: 10.1007/s11243-006-0132-z

Hosny N. M. 2009. Synthesis and Charcterization of Transition Metal Complexes Derived from (E)-(N)-(1-(Pyridine-2-yl)ethylidiene)benzohydrazide (PEBH). *Journal Molecular Structure*, 923:98**.** doi.org/10.1080/15533174.2011.591296

Hosny N. M. 2010. Cu(II) and Zr(IV) Complexes with (E)-N-(1-(Pyridine-4-yl)ethylidine)nicotinohydrazide. Synth. React. Inorg-Org Met Nano 6: 391. doi:10.1080/15533174.2010.492550

Hosny N. M., El Morsy E. A., Sherif Y. E. 2015. Synthesis, spectral, optical and anti-inflammatory activity of complexes derived from 2-aminobenzohydrazide with some rare earths. *Journal of Rare Earths*, 33: 758. doi.org/10.1016/S1002-0721(14)60482-8

Hosny N. M., Hussien M. A., Radwan F. M., Nawar N**.** 2014. Synthesis, spectral characterization and DNA binding of Schiff-base metal complexes derived from 2-amino-3-hydroxyprobanoic acid and acetylacetone. *Spectrochimica Acta A*, 132: 121. doi:10.1016/j.saa.2014.04.165

Hosny N. M., Shallaby A. M. 2007. Spectroscopic Characterization of Some Metal Complexes Derived from 4-Acetylpyridine Nicotinoylhydrazone, *Transition Metal Chemistry*, 32:1085. Doi: 10.1007/s11243-007-0288-1

Hosny N. M., Sherif Y. E. 2015. Synthesis, structural, optical and anti-rheumatic activity of metal complexes derived from (E)-2-amino-N-(1-(2-aminophenyl)ethylidene) benzohydrazide (2-AAB) with Ru(III), Pd(II) and Zr(IV). *Spectrochimica Acta A.,* 136:510. doi.org/10.1016/j.saa.2014.09.064

Hussain J., Chakravrty A. R. 2012. Photocytotoxic lanthanide complexes, *Journal of Chemical Science*, 124:1327.

Hussien M. A., Nawar N., Radwan F. M., Hosny N. M. 2015. Spectral characterization, optical band gap calculations and DNA binding of some binuclear Schiff-base metal complexes derived from 2-amino-ethanoic acid and acetylacetone, J. Mol. Struct., 1080:162. doi.org/10.1016/j.molstruc.2014.09.071

Hyperchem 7, developed by Hypercube Inc. 2002.

Jain A., Jain S. K., Ganesh N. 2010. Design and development of ligand-appended polysaccharidie nanoparticles for the delivery of oxaliplatin in colorectal cancer, *Nanomedicine Nanotechnology Biology and Medicine,* 6: 179. DOI:10.1016/j.nano.2009.03.002

Kostova I. 2006. Platinum complexes as anticancer agents, *Recent Patents on Anti-Cancer Drug Discovery,* 1:1.

Lever A. B. P. 1986. Inorganic electronic spectroscopy, Elsevier, Amsterdam.

Levesque R. 2007. SPSS: Programming and Data Management: A Guide for SPSS and SAS users, Fourth Edition, SPSS INC , Chicago III.

Luo L. J., Tao W., Hu X. Y., Xiao T., Heng B. J., Huang W., Wang H., Han H. W., Jiang Q. K., Wang J. B., Tan Y. W. 2011. Mesoporous F-doped ZnO prism arrays with significantly enhanced photovoltaic performance for dye-sensitized solar cells. *Journal of Power Sources,* 196: 10518. doi.org/10.1016/j.jpowsour.2011.08.011

McLiman W. F., Dairs E. V., Glover F. L., Rake G. W. 1957. The submerged culture of mammalian cells; the spinner culture, *Journal of Immunology*, 79:428. PMID:13491853

Meier J., Theakston R. D. 1986. Approximate LD50 determinations of snake venoms using eight to ten experimental animals. *Toxicon Journal*, 24:395. PMID:3715904

Misbah ur Rehman, Imran M., Arif M. 2013. Synthesis, Characterization and in vitro Antimicrobial studies of Schiff-bases derived from Acetylacetone and amino acids and their oxovanadium(IV) complexes. *American Journal of Applied Chemistry*, 1: 59. doi: 10.11648/j.ajac.20130104.13

Mohammadikish M. 2014. Green synthesis and growth mechanism of new nanomaterial: Zn (salen) nano-complex. *Crystal Engineering Communication,* 16:8020.doi.org/10.1016/j.jcrysgro.2015.08.029

Mujahid M., Kia A. F., Duff B., Egan D. A., Devereux M., McClean S., Walsh M., Trendafilova N., Georgieva I., Creaven B. S. 2015. Spectroscopic studies, DFT calculations, and cytotoxic activity of novel silver(I) complexes of hydroxy ortho-substituted-nitro-2H-chromen-2-one ligands and a phenanthroline adduct. *Journal Inorganic Biochemistry*,153:103.doi:10.1016/j.jinorgbio.2015.10.007

Nakamoto K., (ed). (1970) Infrared spectra of inorganic and coordination compounds. John Wiley, New York.

Noordhui P., Laan A., Born K., Losekoot N., Kathmann I., Peters G. 2008. Oxaliplatin activity in selected and unselected human ovarian and colorectal cancer cell lines. *Biochemical Pharmacol ogy,* 76: 53. doi:10.1016/j.bcp.2008.04.007

Philips S., Rista S., Dominic S., Anne M., Jaames M., David V., Jonathan T. W., Heidi B., Susan K., Michael R. B. 1990. Newcoloremtric cytotoxicity assay for anti-cancer drug screening. *Journal of National Cancer Institute,* 8:1107. doiI:10.1016/j.bcp.2008.04.007

Sakurai H., Kojima Y., Yoshikawa Y., Kawabe K., Yasui H. 2002. Antidiabetic vanadium(IV) and zinc(II) complexes. *Coordination Chemistry Review,* 226: 187. doi.org/10.1016/S0010-8545(01)00447-7

Sherif Y. E., Hosny N. M. 2014. Synthesis, characterization, and anti-rheumatic potential of phthalazine-1,4-dione and its Cu(II) and Zn(II) complexes, *Medicinal Chemistry Research*, 23:2536**.** doi: 10.1007/s00044-013-0827-6

Sherif Y. E., Hosny N. M. 2014. Anti-rheumatic potential of ethyl 2-(2-cyano-3-mercapto-3-(phenylamino) acrylamido)-4,5,6,7-tetrahydrobenzo[b]thiophene-3-carboxylate and its Co(II),

372 Cu(II) and Zn(II) complexes, *European Journal of Medicinal Chemistry,* 83: 338.
373 doi.org/10.1016/j.ejmech.2014.06.038

374 **Sönmez M.**, Celebi M., Yardim Y., Sentürk Z. 2010. Palladium(II) and platinum(II) complexes a
375 symmetric Schiff base derived from 2,6,diformyl-4-methylphenol with N-aminopyrimidine:
376 Synthesis, characterization and detection of DNA interaction by voltammetry, *European Journal of*
377 *Medicinal Chemistry*, 45: 4215. doi: 10.1016/j.ejmech.2010.06.016.

378 **Tabrizi L.**, Chiniforoshan H. 2017. Cytotoxicity and cellular response mechanisms of water-
379 soluble platinum(II) complexes of lidocaine and phenylcyanamide derivatives. *BioMetals*,
380 30:59. doi:10.1007/s10534-016-9986-5

381 **Wang B.,** Wang Z., Ai F., Tang W. K., Zhu G. 2015. A monofunctional platinum(II)-based
382 anticancer agent from a salicylanilide derivative: Synthesis, antiproliferative activity, and
383 transcription inhibition, *Journal of Inorganic Biochemistry*. 142: 118.
384 doi.org/10.1016/j.jinorgbio.2014.10.003

385 **Wang Q.,** Yang L., Wu J., Wang H., Song J., Tang. X. 2017. Four mononuclear platinum(II)
386 complexes: Synthesis, DNA/BSA binding, DNA cleavage and cytotoxicity. *BioMetals*, 30:17.
387 doi:10.1007/s10534-016-9984-7

388 **Zhukova O. S.,** Dobrynin I.V. 2001. Current results and perspectives of the use of human tumor
389 cell lines for antitumor drug screening. *Voprosy Onkologii*, 47: 706. PMID:11826493

390

391 Supporting Informations

392

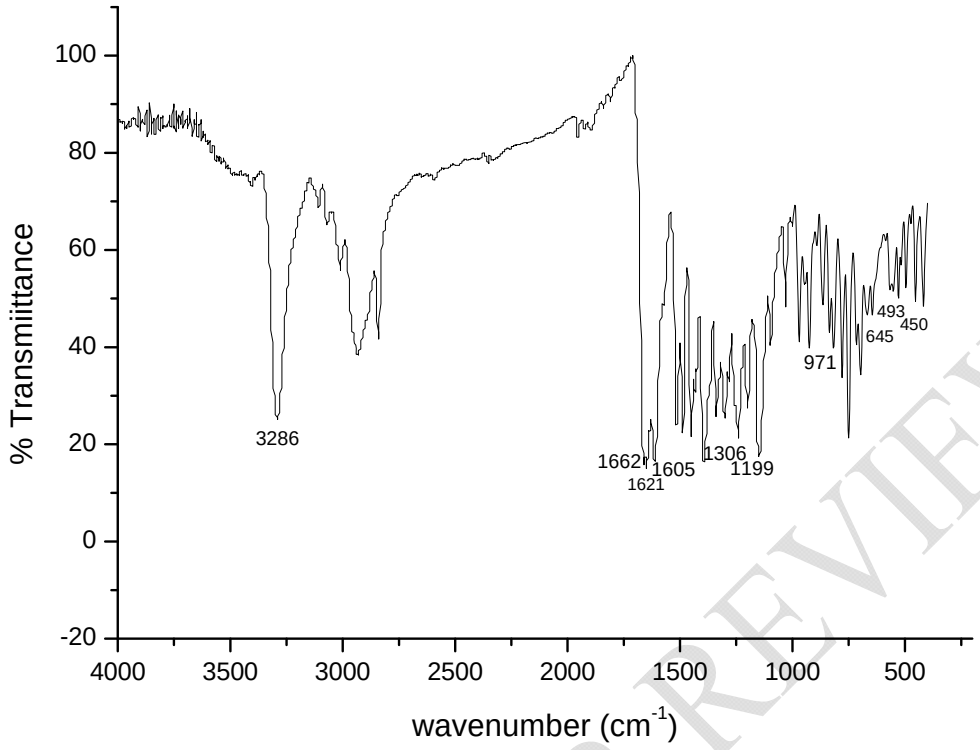

Fig. S1. IR spectrum of the ligand

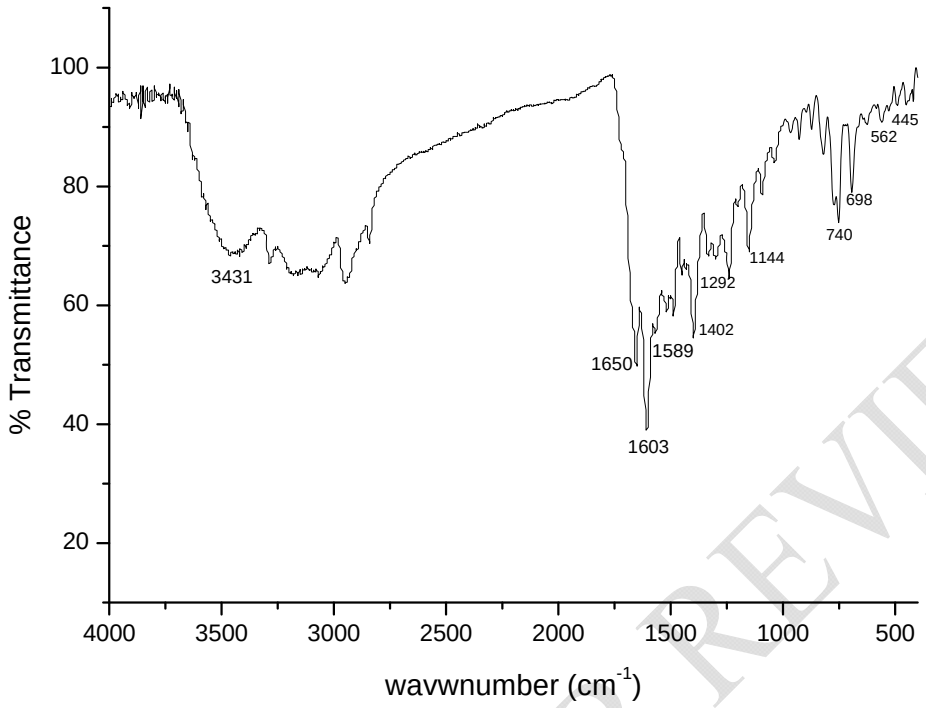

Fig. S2. IR spectrum of Pt(II) complex

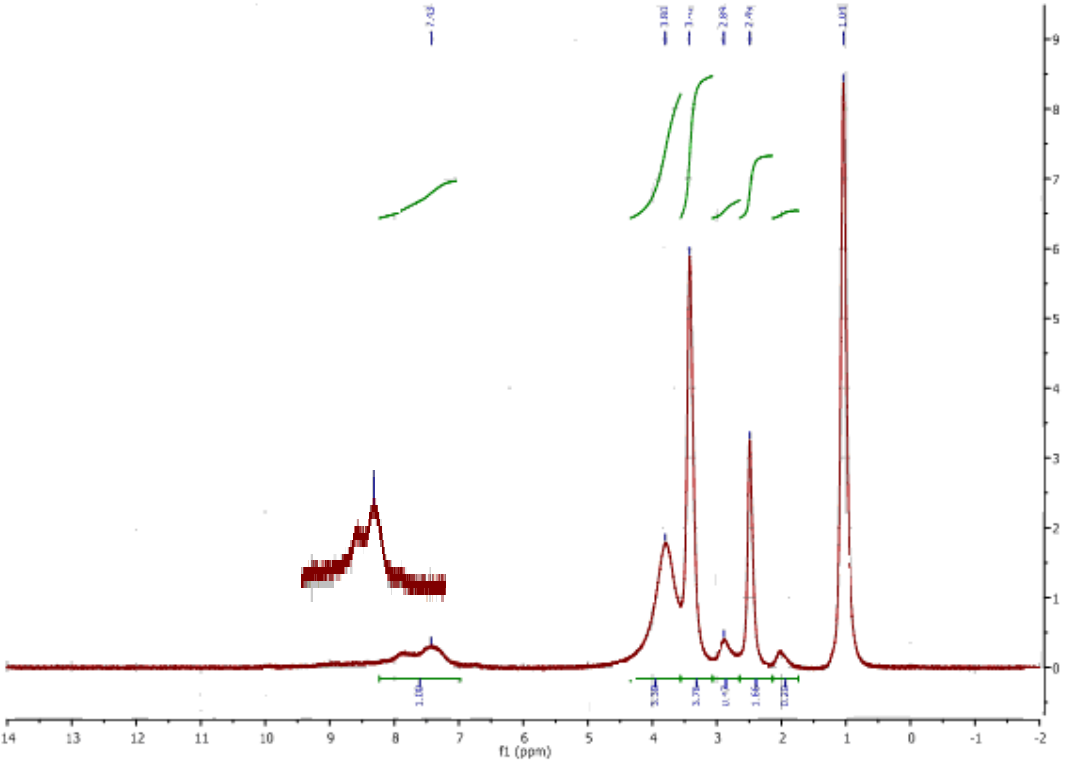

Fig. S3. ^{1}HNMR spectrum of Pt(II) complexes